Dielectric Lens Antenna for Industrial Radar Applications

Lajos Nagy, *Member, IEEE*

***Abstract*—Industrial radar applications like tank level measurement is an important research and application area in radar technology. Radar level measurement is a safe solution even under extreme process conditions (pressure, temperature) and vapors. Special antennas are required to meet electromagnetic requirements such as high gain, low sidelobe level and high bandwidth. The small side-beam level and narrow main beam primarily minimize reflections from the side of the tank, while the bandwidth determines the distance resolution of the measurement system. Another requirement is a small size and good manufacturability of the antenna.**

The main promising solutions are the use of microstrip, horn or dielectric lens antennas for tank level measurement systems. After several tests, we have concluded that the optimal choice for tank level radar measurement task, in terms of integrability and antenna parameters, is a dielectric antenna. The dielectric antenna has many other applications in modern mobile systems as 5 and 6 G systems where these antennas are elements of antenna arrays of beamforming or MIMO systems.

In this paper, a special dielectric lens antenna is presented, satisfying main requirements, namely a circular antenna cross section, high antenna aperture efficiency and low sidelobe level.

The center frequency of the antenna is 26 GHz with a bandwidth of 1 GHz. The paper presents the analytic investigation and design of the dielectric lens antenna and the circular waveguide transition in detail. The electromagnetic design of the antenna was carried out using CST Microwave Studio 3D software.

***Index Terms*—Radar, antenna, lens antenna, 5G**

INTRODUCTION

Product quality check, operational safety, and economic efficiency can only be ensured by continuous measurements and control systems based on these measurements for the most important areas, which are the oil industry, transport. Liquids, pastes, bulk solids, and liquefied gases are most often stored in tanks, silos, or mobile containers. These tanks are used in the chemical and petrochemical industries, the pharmaceutical and life sciences industries, the water industry, the chemical and petrochemical industries, the water and wastewater, and the food industries.

There are several classical and modern methods for measuring the product level in process and storage tanks. Applications are in the chemical, petrochemical, pharmaceutical, water, and food industries, mobile tanks on vehicles and ships, and natural reservoirs such as seas, dams, lakes, and oceans. Typical tank heights for these applications are in the range from 0.5 m to 37 m.

Lajos Nagy, is with Budapest University of Technology and Economics, Budapest, Hungary, Department of Broadband Infocommunications and Electromagnetic Theory, Faculty of Electrical Engineering (E-mail: nagy.lajos@vik.bme.hu).

DOI: 10.36244/ICJ.2024.3.7

In practical applications two main measurement tasks can be distinguished:

- continuous level measurement, i.e., level indication,
- level detection, i.e., detection of an alarm limit to prevent overfilling.

Many level measurement devices are mounted on top of the tank and measure primarily the distance between their mounting position and the product's surface (Fig. 1).

For level measurement, a significant number of different principles measurement techniques are available [1], and it is advisable to select the optimum technique and sensor.

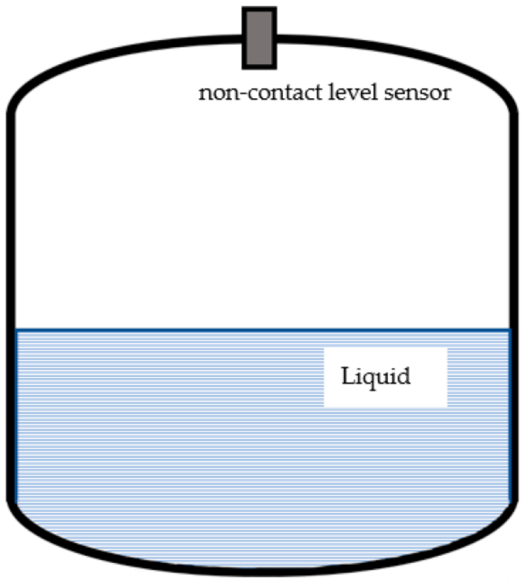

Fig. 1. Tank with liquid and non-contact sensors on the top of the tank

The commonly used tank-level measurement methods are based on the next basic principles:

buoyant object floats, RF capacitance, radar, ultrasonic, and hydrostatic head/tank gauging.

No single principle applies to all measurement areas. Therefore, measurement systems should be selected based on what works reliably under the given conditions, and at the same time meet the accuracy of the measurement.

We developed a sensor antenna for radar-level pulse measurement, which is based on the principle that the time required for the propagation of microwaves. It is the time takes for the wave packet to travel during the entire round trip between the non-contact transducer detected material level and the measuring device. Pulse radar has been widely used for distance measurement since the early days of radar. Radar level measurement is a safe non-contact solution even under extreme process conditions, at high pressure, and temperature, vapors. For radar measurements, special antennas are required to meet electromagnetic requirements such as high gain, low sidelobe level, and high bandwidth.[2]

Another requirement is a small size and good manufacturability of the antenna. (Fig. 2)

Fig. 2. Standard level meter house

Many antenna types are promising for contactless tank-level radar measurements, such as conical horn antennas, parabolic reflector antennas, dielectric antennas [3–6] and microstrip antennas.

Recently, theoretical work is conducted applying metamaterial-based antennas [7] also for tank-level measuring sensor antennas. These analytical or numerical solutions allow for the designing and building of useful antennas and devices; however, more effective fabrication techniques need to be developed for these devices. Another difficulty of the metamaterial type antennas is the bandwidth because these devices show generally narrowband behavior and bandwidth is not analyzed [7].

In this paper, a special dielectric antenna was designed, that meets the main requirements, i.e., high gain, low sidelobe level, high bandwidth, and good manufacturability of the antenna.

CST Microwave Studio was used to simulate and fine-tune the antenna.

I. ANTENNA CONSTRUCTION

The antenna consists of three main parts. These are: (Fig.3)

- coaxial to circular waveguide transition,
- air filled to dielectric filled circular waveguide transition,
- dielectric antenna.

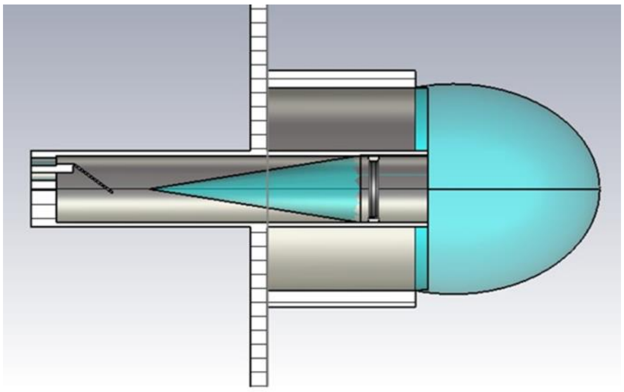

Fig. 3. Dielectric antenna construction

The first part (coaxial to circular waveguide transition) of the construction is not under examination, now we focus on the air filled to dielectric filled circular waveguide transition and dielectric antenna.

I.1 Analysis and design of the dielectric lens

Dielectric lens antennas are attracting a renewed interest for millimeter- and submillimeter wave applications where they become compact, especially for configurations with integrated feeds usually referred as integrated lens antennas. [8-11] Recent research and developments are looking at 5G and Terahertz applications of dielectric antennas. [12-13]

Lenses are very flexible and simple to design and fabricate, being a reliable alternative at these frequencies to reflector antennas. Lens target output can range from a simple collimated beam (increasing the feed directivity) to more complex multi-objective specifications.

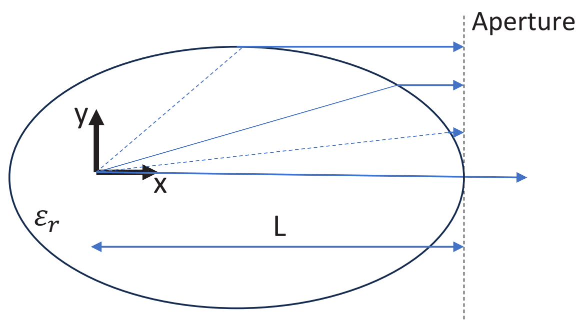

Fig. 4. Rays from excitation point to the aperture.

The operating mechanism of dielectric antennas is most easily investigated by ray tracing or geometrical optics. In Fig 4 we have plotted some ray paths between the source point and the antenna aperture.

Using Fig. 4 it can be express the propagation time from excitation point to any point of the aperture as

$$t = \frac{L}{v} = \frac{\sqrt{x^2 + y^2}}{v} + \frac{L - x}{c} \quad (1)$$

where the phase velocity in the dielectric with relative dielectric constant ε_r is

$$v = \frac{c}{\sqrt{\varepsilon_r}}$$

where
c is the speed of light in air.

The uniform phase on aperture requires the same propagation time and using this the following expression will be given.

$$y^2 = L^2 \frac{(\sqrt{\varepsilon_r} - 1)^2}{\varepsilon_r} + 2xR\frac{\sqrt{\varepsilon_r} - 1}{\varepsilon_r} + x^2\left(\frac{1}{\varepsilon_r} - 1\right) \quad (2)$$

It can be found, that the equation (2) is equation of an ellipse, and the excitation point is the focal point of it.
Ellipse semi axes are:

$$B = R$$

$$A = R\frac{\sqrt{\varepsilon_r}}{\sqrt{\varepsilon_r - 1}}$$

The distance of the focal point and aperture, L is:

$$L = \left(\sqrt{\varepsilon_r} + 1\right)\frac{R}{\sqrt{\varepsilon_r - 1}} \quad (3)$$

Finally, we can express the ellipse equation using the semi axis B=R as

$$y^2 = \frac{\varepsilon_r - 1}{\varepsilon_r}\left[R^2 + \frac{2xR}{\sqrt{\varepsilon_r - 1}} - x^2\right] \quad (4)$$

The dielectric lens is made of teflon (Politetrafluoretilén, FTFE), with a relative dielectric constant $\varepsilon_r = 2.1$. (Fig. 5)
After defining the geometry that ensures a uniform phase distribution, in the next section we calculate the aperture electric field illumination distribution, also using the geometrical optical principle.

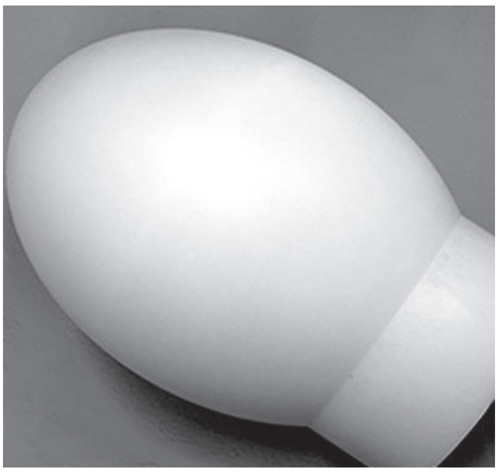

Fig. 5. Elliptic dielectric antenna.

I.2 *Aperture field distribution analysis using Geometrical Optics*

The aperture field distribution analysis will be based on classical reflector radiation characteristic analysis. There are two basic techniques for the analysis of the radiation characteristics of reflectors. One is called the current distribution method, which is a physical optics (PO) approximation. With the aperture distribution method, the field is found first over a plane, which is normal to the reflector's axis, and lies at its focal point (the antenna aperture). Geometrical Optics (ray tracing) will be used to determine that.

In the case of our dielectric antenna the GO approximation can be used. It is assumed that the equivalent sources are zero outside the dielectric antenna's aperture, which is a circle with radius R (Fig. 6).

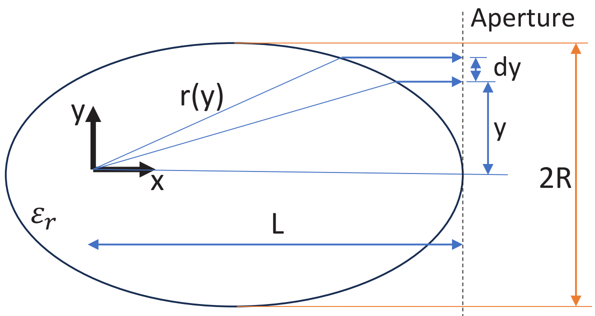

Fig. 6. GO analysis of elliptic dielectric antenna.

The field distribution at the aperture of the ellipse antenna is necessary to find, to calculate the far-field pattern, directivity. Since all rays from the feed travel the same time to the aperture, the aperture distribution is of uniform phase. However, there is a non-uniform amplitude distribution. This is because the power density of the rays leaving the feed falls off as $1/r^2$. After the refraction, there is practically no spreading loss since the rays are collimated (parallel).

GO assumes that the power density in free space follows straight paths. Applied to the power transmitted by the feed the power in a conical wedge, stay confined within as it progresses along the cone's axis.

The aperture field distribution can be expressed as

$$E_a \sim \frac{1}{r(y)} \quad (5)$$

where E_a is the electric field strength on aperture.
The distance of refraction r(y) is as follows.

$$r(y) = \sqrt{x^2 + y^2} = \sqrt{[f^{-1}(y)]^2 + y^2} \quad (6)$$

where

$$x = f^{-1}(y) = \frac{R}{\sqrt{\varepsilon_r - 1}}\left[1 - \sqrt{\varepsilon_r}\frac{\sqrt{R^2 - y^2}}{R}\right]$$

The aperture illumination is rotationally symmetrical and depends only on radial distance on the aperture. (Fig.7.)

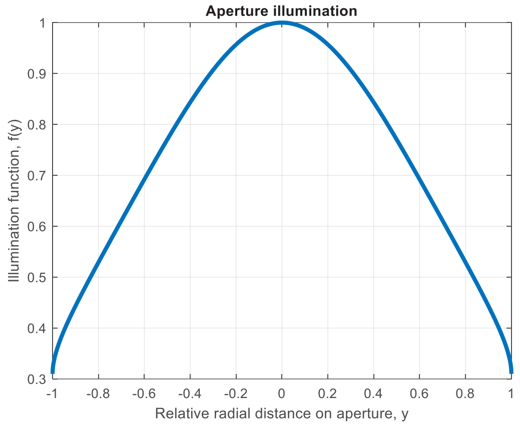

Fig. 7. Aperture illumination

Fig. 7 clearly shows that the distribution electric field illumination function of the aperture decreases towards the edges, resulting in a favorable decrease of the sidelobe level.

The aperture far field approximation using the illumination function as follows.

$$E(\underline{r}) = j\frac{2\pi}{\lambda}E_0\frac{e^{-j\beta r}}{r}\frac{(1+cos\vartheta)}{2}\int_0^R f(y)\cdot J_0(\beta\ y\ sin(\vartheta))\ y\ dy \qquad (7)$$

where

$E(\underline{r})$ the far field electric field strength,
$\underline{r}$ position vector of observation point, from origin,
λ free space wavelength,
E_0 aperture field maxima,
$f(y)$ aperture illumination as function of radial distance y,
β free space phase constant,
J_0 Bessel function of first kind,
ϑ angle of observation point, from origin.
$(1+cos\vartheta)/2$ Huygens wavelet characteristics

The antenna far field directional characteristics were calculated using Matlab script. (Fig. 8)

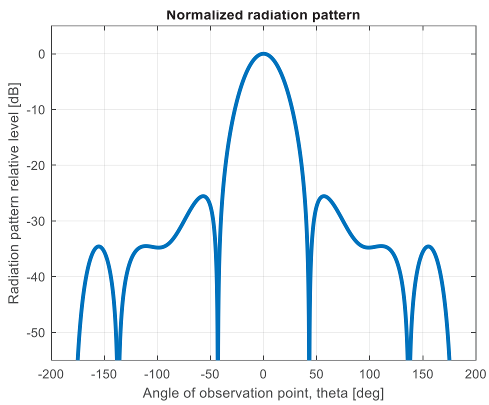

Fig. 8. Aperture far field radiation pattern plane cut

The most important antenna characteristics that can be read from the directional characteristics (Fig. 8) are the main lobe beam width and the sidelobe suppression.

II. AIR TO DIELECTRIC CIRCULAR WAVEGUIDE TRANSITION

In the design of the air dielectric transition, the most important considerations are low reflection and low attenuation, and to ensure unchanged propagation of the excitation mode.

Traditionally, the excitation is provided by a probe, formed from a coaxial connector, and the transition is a continuous dimensional transition, which in the case of a circular feed line means a linear tapered transition.

The main elements of this section are shown in the Fig. 9, 10 and 11.

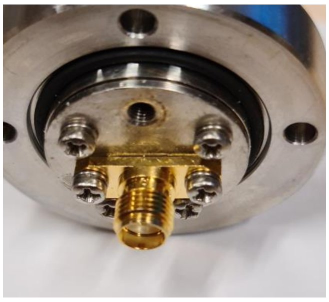

Fig. 9. Coaxial SMA connector attached to the circular waveguide

Fig. 10. Circular waveguide to dielectric antenna.

Fig. 11. Conical transition (linear taper) of air to dielectric in circular waveguide.

To perform the analysis, we built a CST model to study the linear tapered conical transition (Fig. 12) and to compare exponential taper (Fig. 13).

The lengths of the structure investigated are 40 mm and only the transition section lengths differ.

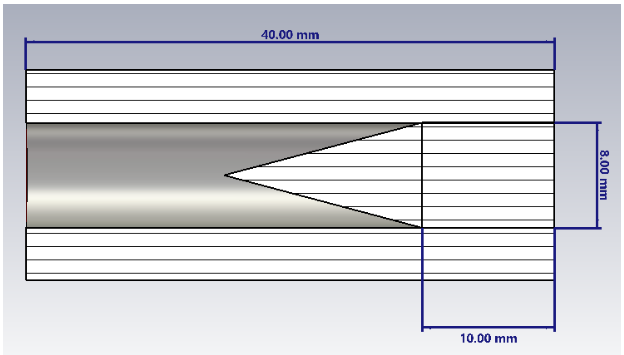

Fig. 12. Conical (linear taper) transition

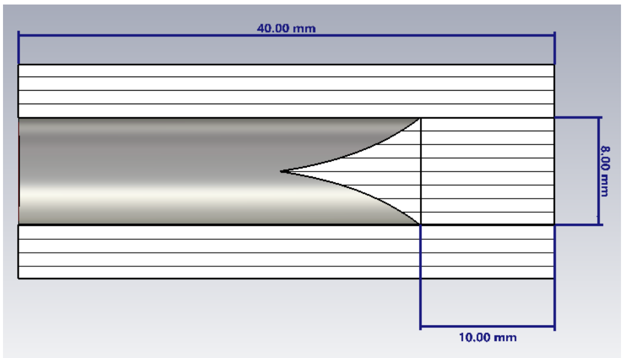

Fig. 13. Exponential taper transition

The S11 reflection coefficient was investigated and compared to the linear (Fig. 14) and exponential (Fig. 15) tapered transitions.

L_c is the length of transition section, which is the parameter of parametric analysis.

As can be seen in the figures, significantly shorter transitions were considered for the exponential transitions and still a significant improvement over linear tapers can be achieved.

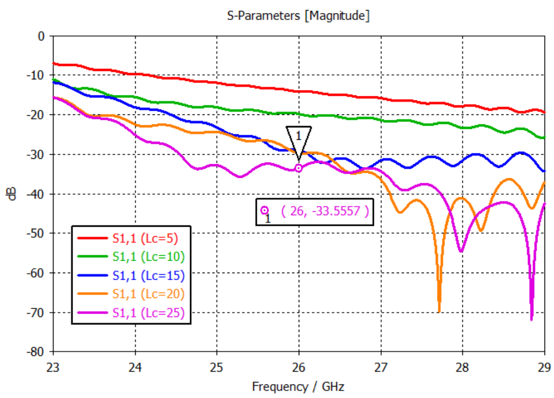

Fig. 14. Reflection coefficient of the linear tapered transition.

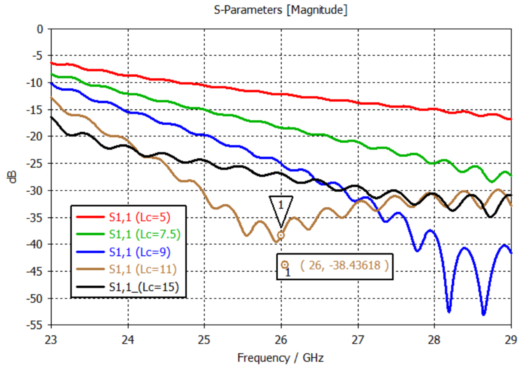

Fig. 15. Reflection coefficient of the exponential tapered transition.

The frequency band of the antenna design is the 25.5-26.5 GHz band, and in this range, by applying the exponential transition, we achieved 5 dB improvement in the reflection coefficient using only 11 mm exponential transition length instead of 25 mm for linear tapered one.

III. RESULTS

Using the experience gained so far, a CST electromagnetic model of the final dielectric antenna has been constructed for each of the taper investigated.

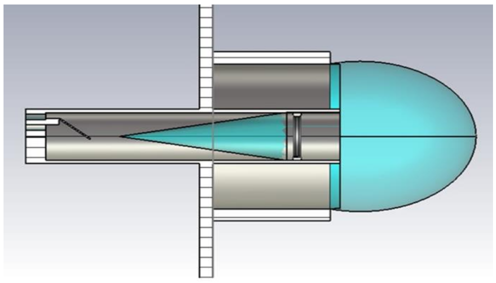

Fig. 16. Elliptical dielectric antenna with linear tapered air to dielectric transition.

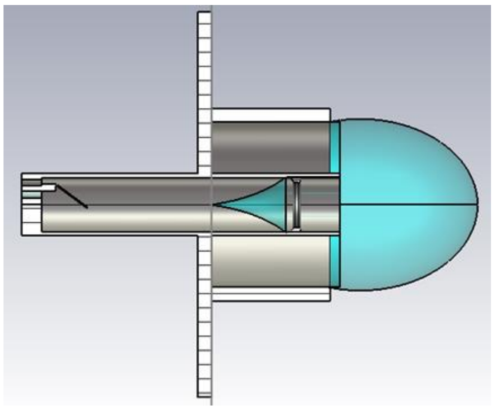

Fig. 17. Elliptical dielectric antenna with exponential tapered air to dielectric transition.

The dimensions of both antennas are identical, the only difference is the transition taper and its length. (Fig. 16 and 17)

The Fig. 18 shows the comparison of input reflection of the dielectric elliptic antenna with two transitions investigated. The antenna with exponential tapered transition shows at least 5 dB of reflection decrease in antenna design 25.5-26.5 GHz band. This result is in good agreement with the similar result obtained in the transition study in chapter II.

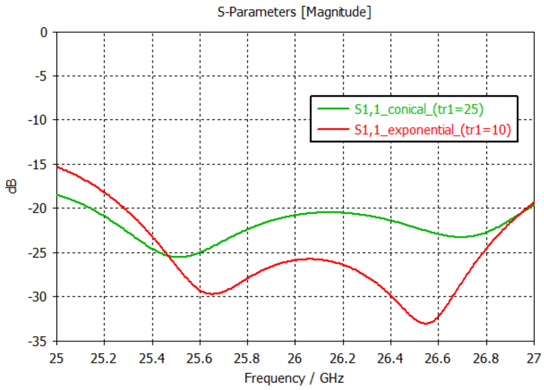

Fig. 18. Input reflection of elliptical dielectric antenna with linear and exponential tapered air to dielectric transition.

Reducing the input reflection is only one of the beneficial properties of the exponential transition, it also offers the possibility to reduce the overall power line length, which will be investigated in further research.

The antenna far field pattern has been investigated at the center frequency of the design is the 25.5-26.5 GHz band, at 26 GHz. (Fig. 19)

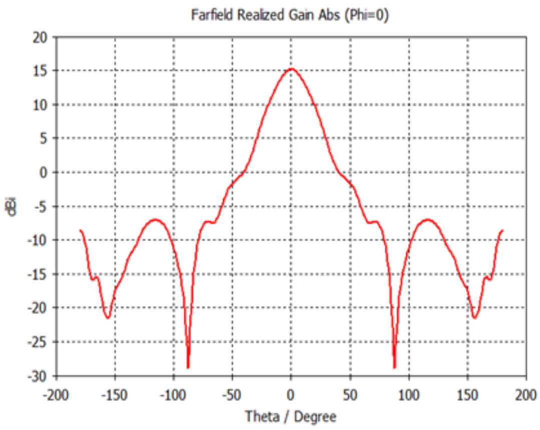

Fig. 19. Radiation pattern plane cut of elliptical dielectric antenna with exponential tapered air to dielectric transition.

The dielectric elliptical antenna diameter is d=24 mm, therefore the geometrical aperture area is

$$A_{geom} = \left(\frac{d}{2}\right)^2 \pi = 452mm^2 \quad (8)$$

The antenna gain is G=15 dB can be determined from Fig. 19.

Based on this the antenna effective area is [14]

$$A_{eff} = \frac{\lambda^2}{4\pi} G = 335mm^2 \quad (9)$$

According to the standard definition, Aperture efficiency of an antenna, is the ratio of the effective radiating area (or effective area) to the physical area of the aperture. Therefore, the antenna aperture efficiency is:

$$\eta = \frac{A_{eff}}{A_{geom}} = 74\%$$

Aperture efficiencies of typical aperture antennas vary from 0.35 to over 0.70, so the dielectric elliptic antenna designed has a quite significant.

As a final investigation the analytic radiation pattern plane cut was compared to the simulated result. (Fig. 20)

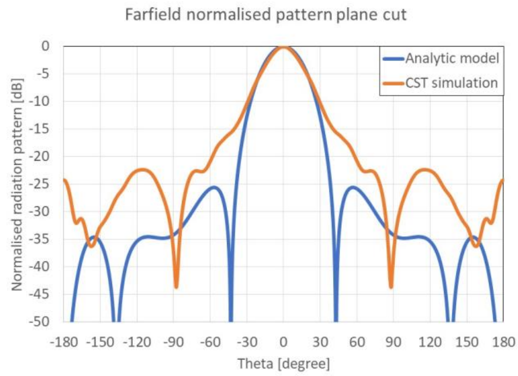

Fig. 20. Radiation pattern plane cut of elliptical dielectric antenna (Analytic and simulated results).

Main results of the comparison

the analytic model gives a quite similar result for the main beam,

the analytic model underestimates the side lobe levels.

The analytic model therefore can be used for determining the 3 dB beamwidth, which is a good starting parameter to estimate the antenna directivity. On the other side the side lobe level has also influence on directivity.

The main reasons of the differences

analytic model uses simplified radiation model for wavelets, the Huygens elementary radiator,

instead of excitation point, the open circular waveguide field is more difficult than an isotropic radiator.

Using Fresnel-Kirchoff wavelet element model, the radiation pattern estimation can be improved, but the finite size open circular waveguide excitation can be taken account only by using either more difficult analytic model or by numerical field solver like CST. [15]

IV. OTHER APPLICATIONS OF DIELECTRIC ANTENNAS

Another important application of dielectric antennas is as base station antennas for new generation mobile systems and automotive radar antenna systems. The main difference in this application is that the dielectric antenna is used as an element of an antenna system, which can be beamforming system [16, 17] or MIMO system.

The [16] introduces linearly polarized flat lens antenna (LP-FLA) for 5G system and [17] a microstrip patch feed dielectric lens antenna for automotive radar.

Comparing the results of the present design with antennas proposed in [16, 17] can be concluded that the main parameters of the antennas are the following.

TABLE I
ANTENNA APERTURE EFFICIENCY AND SIDE LOBE LEVEL

Ref	Aperture Efficiency	Side Lobe Level
5G [16]	60%	-20 dB
Automotive radar [17]	10%	-16 dB
Present design	74%	-18 dB

It can be concluded that the proposed elliptical steering curve antenna provides a similar side beam level with better aperture efficiency, which is one of the most important aspects.

V. CONCLUSION

We presented a systematic design of a dielectric antenna for microwave tank-level measurement radar system. The antenna optimally fills the opening of the tank (Fig 1 and 2), therefore maximal gain can be reached. The plane wave aperture illumination ensures the improved sidelobe level to reduce the side reflections from tank sidewalls. Detailed analysis of aperture illumination and radiation pattern are introduced.

The main contribution of the article is introduction of the complete design and analysis of a dielectric antenna for radar and communications applications. We also optimized a new air to dielectric circular waveguide transition with which the matching has been improved by 5 dB in the working frequency band.

Finally, the theoretical (analytical) radiation pattern is compared to the simulated one.

We plan to finalize the antenna prototype and perform radiation pattern measurements. Also 80 GHz band antenna design and measurement are our next plans.

ACKNOWLEDGMENT

The author very much appreciates the support from the NIVELCO Process Control Co. and the infrastructure of the Department of Broadband Infocommunication and my colleague, Ferenc Lénárt from Antenna Laboratory of Electromagnetic Theory at the Budapest University of Technology and Economics.

This research was funded by the Hungarian Fund 2020-1.1.2-PIACI-KFI-2021-00278.

REFERENCES

[1] G. Vass, “The Principles of Level Measurement,” Available online: https://www.fierceelectronics.com/sensors/bmws-i-vision-dee-concept-car-can-talk-and-offers-32-swappable-exterior-colors (accessed on 15 December 2022)

[2] Advanced 80 GHz Radar Level Transmitters, Nivelco Process Control Co., https://www.nivelco.com/us/news?id=new_w200

[3] G. Armbrecht, C. Zietz, E. Denicke, and I. Rolfes, “Antenna Impact on the Gauging Accuracy of Industrial Radar Level Measurements,” *IEEE Trans. Microwave Theory Tech*., vol. 59, no. 10, pp. 2554–2562, 2011.

[4] Gerding, M.; Much, T.; Nils, P. Dielectric Antenna. *U.S. Patent* 8,242,965, 14 August 2012. Available online: https://patents.justia.com/patent/8242965 (accessed on 15 December 2022).

[5] N. Pohl, “A dielectric lens antenna with enhanced aperture efficiency for industrial radar applications,” in *Proc. IEEE Middle East Conf. Antennas and Propagation (MECAP)*, 2010

[6] N. Pohl, “Dielektrische Antenne,” *German Patent Application Publication* DE102008008715A1, Aug. 13, 2009

[7] Palmeri, R.; Bevacqua, M.T.; Morabito, A.F.; Isernia, T. Design of Artificial-Material-Based Antennas Using Inverse Scattering Techniques. *IEEE Trans. Antennas Propag*. 2018, 66, 7076–7090.

[8] A. Net, S. Maci and P. J. l. de Maagt, “Reflections inside an elliptical dielectric lens antenna”, *IEE Proceedings Microwaves, Antennas and Propagation*, vol 145, no. 3, pp 243–247, Jun 1998.

[9] N. T. Nguyen, R. Sauleau, and C. J. M. Perez, “Very Broadband Extended Hemispherical Lenses: Role of Matching Layers for Bandwidth Enlargement,” *IEEE Trans. Antennas Propagat*., vol. 57, no. 7, pp. 1907–1913, 2009

[10] I. Abdo, T. Fujimura, T. Miura, A. Shirane and K. Okada, "A 300GHz Dielectric Lens Antenna," *2019 12th Global Symposium on Millimeter Waves (GSMM)*, Sendai, Japan, 2019, pp. 17–19, DOI: 10.1109/GSMM.2019.8797658.

[11] T. Komljenovic and Z. Sipus, "Dielectric lens antennas design at millimeter waves," *2008 50th International Symposium ELMAR*, Borik Zadar, Croatia, 2008, pp. 621–624.

[12] K. Rasilainen, J. Chen, M. Berg and A. Pärssinen, "Dielectric Lens Antennas for 300-GHz Applications," *2021 15th European Conference on Antennas and Propagation (EuCAP),* Dusseldorf, Germany, 2021, pp. 1–5, DOI: 10.23919/EuCAP51087.2021.9411358.

[13] K. Konstantinidis et al., “Low-THz dielectric lens antenna with integrated waveguide feed,” *IEEE Trans. THz Sci. Technol.*, vol. 7, no. 5, pp. 572–581, Sep. 2017.

[14] Balanis, Constantine A. *Antenna Theory: Analysis and Design*. 3rd ed. Hoboken, NJ: John Wiley, 2005.

[15] CST Studio, https://www.3ds.com/products/simulia/cst-studio-suite

[16] Asrin Piroutiniya et. al., “Beam Steering 3D Printed Dielectric Lens Antennas for Millimeter-Wave and 5G Applications”, August 2023, *Sensors* 23(15):6961, DOI: 10.3390/s23156961

[17] P. Wenig, R. Weigel and M. Schneider, "A dielectric lens antenna for digital beamforming and superresolution DOA estimation in 77 GHz automotive radar," *2008 International ITG Workshop on Smart Antennas*, Darmstadt, Germany, 2008, pp. 184–189, DOI: 10.1109/WSA.2008.4475557.

Lajos Nagy He received the Engineer option Communication) and PhD degrees, both from the Budapest University of Technology and economics (BME), Budapest, Hungary, in 1986 and 1995, respectively. He joined the department of Microwave Telecommunications (now Broadband Infocommunications and Electromagnetic Theory) in 1986, where he is currently an associate professor. He is a lecturer on graduate and postgraduate courses at BME on Antennas and radiowave propagation, Radio system design, Adaptive antenna systems and Computer Programming. His research interests include antenna analysis and computer aided design, electromagnetic theory, radiowave propagation, communication electronics, signal processing and digital antenna array beamforming, topics where he has produced more than 100 different book chapters and peer-reviewed journal and conference papers. Member of Hungarian Telecommunication Association, official Hungarian Member and Hungarian Committee Secretary of URSI, Chair of the IEEE Chapter AP/ComSoc/ED/MTT.